



Mamba as Decision Maker: Exploring Multi-scale Sequence Modeling in Offline Reinforcement Learning

Jiahang Cao^{1*}, Qiang Zhang^{1*}, Ziqing Wang², Jingkai Sun¹, Jiaxu Wang¹, Hao Cheng¹,
Yecheng Shao⁴, Wen Zhao³, Gang Han³, Yijie Guo³, Renjing Xu^{1†}

Abstract—Sequential modeling has demonstrated remarkable capabilities in offline reinforcement learning (RL), with Decision Transformer (DT) being one of the most notable representatives, achieving significant success. However, RL trajectories possess unique properties to be distinguished from the conventional sequence (e.g., text or audio): (1) local correlation, where the next states in RL are theoretically determined solely by current states and actions based on the Markov Decision Process (MDP), and (2) global correlation, where each step’s features are related to long-term historical information due to the time-continuous nature of trajectories. In this paper, we propose a novel action sequence predictor, named Mamba Decision Maker (MambaDM), where Mamba is expected to be a promising alternative for sequence modeling paradigms, owing to its efficient modeling of multi-scale dependencies. In particular, we introduce a novel mixer module that proficiently extracts and integrates both global and local features of the input sequence, effectively capturing interrelationships in RL datasets. Extensive experiments demonstrate that MambaDM achieves state-of-the-art performance in Atari and OpenAI Gym datasets. Furthermore, we empirically investigate the scaling laws of MambaDM, finding that increasing model size does not bring performance improvement, but scaling the dataset amount by $2\times$ for MambaDM can obtain up to 33.7% score improvement on Atari dataset. This paper delves into the sequence modeling capabilities of MambaDM in the RL domain, paving the way for future advancements in robust and efficient decision-making systems.

I. INTRODUCTION

Decision-making in Reinforcement Learning (RL) typically involves learning a mapping from state observations to actions that maximize cumulative discounted rewards. Recently, [1] introduced the Decision Transformer (DT), which leverages the simplicity and scalability of transformer architectures to establish a new paradigm for learning in offline RL. DT reinterprets the decision-making process as a sequence modeling problem, learning a return-conditioned state-action mapping. This approach predicts the necessary

action to achieve a desired return based on a sequence of past returns, states, and actions. Due to its promising performance, this sequence modeling paradigm has been widely applied to various robotics tasks, including manipulation [2], [3], navigation [4], and behavior generation [5].

However, RL trajectories differ from conventional sequences like text or audio, and thus modeling them cannot be treated as a simple sequence modeling task. RL problems are typically defined by a Markov Decision Process (MDP), where state transition probabilities adhere to the Markov property—meaning the probability of transitioning to the next state depends solely on the current state and action, not on past states. Consequently, local correlations between steps in the trajectory sequence are significant and cannot be ignored. Additionally, since time steps are sequential, each step’s features are related to long-term history information, indicating that RL trajectories also exhibit inner global correlations. Therefore, designing a multi-scale model to capture both global and local features of RL trajectories deserves further exploration.

In this paper, we introduce the Mamba Decision Maker (MambaDM), which provides an in-depth study of the effectiveness of the Mamba module within the framework of reward conditional sequence modeling. We innovatively design the Global-local Fusion Mamba (GLOMa) module to capture both local and global features to better understand the inner correlations within RL trajectories, aiming to enhance model performance. Furthermore, we explore the scaling laws of MambaDM in RL tasks. Unlike in NLP, where larger models typically yield better performance, our findings indicate that, in Atari and OpenAI Gym environments, increasing model size does not necessarily enhance results. But providing a larger dataset for MambaDM can bring performance improvement. We also analyze the Mamba module’s ability to capture dependency information by visualizing changes in the eigenvalues of Mamba’s core transition matrix. Extensive experiments demonstrate that MambaDM achieves state-of-the-art performance across multiple tasks, significantly outperforming the Decision Transformer (DT [1]) in Atari and OpenAI Gym task, and exceeding the performance of state space model-based [6], [7] DMamba [8] by up to 75.3%.

Our contributions can be summarized as follows:

- We propose the Mamba Decision Maker (MambaDM), an effective decision-making method that incorporates

[†]Corresponding author; ^{*}Equal contribution.

¹Jiahang Cao, Qiang Zhang, Jingkai Sun, Jiaxu Wang, Hao Cheng, and Renjing Xu are with the Microelectronics Thrust, The Hong Kong University of Science and Technology (Guangzhou), China.
Email: jcao248@connect.hkust-gz.edu.cn, renjingxu@ust.hk

²Ziqing Wang is with the Department of Statistics and Data Science, Northwestern University, USA.

³Wen Zhao, Gang Han and Yijie Guo are with the Beijing Innovation Center of Humanoid Robotics, China.

⁴Yecheng Shao is with the Center for X-Mechanics, Zhejiang University, China.

a novel global-local fusion mamba (GLoMa) module to model RL trajectories from both global and local perspectives.

- We investigate the scaling laws of MambaDM in RL tasks. Our experimental results indicate that the scaling laws of MambaDM do not completely align with those observed in NLP, suggesting that gathering larger and more diverse RL datasets could be a more effective strategy for enhancing performance compared to merely increasing the model size.
- Extensive experiments validate that MambaDM achieves state-of-the-art results in both Atari and OpenAI Gym, significantly outperforming state space model-based DS4 and DMamba. Additionally, our visualization analysis demonstrates MambaDM’s ability to capture both short-term and long-term dependencies, supporting the reliability of the proposed module.

II. RELATED WORK

A. Offline Reinforcement Learning

Reinforcement Learning (RL) is a framework of algorithms that learn through interactions with an environment. The problem is formulated as a Markov Decision Process [9], [10]. RL aims to maximize rewards through interactions with an environment, which is often a time-consuming and expensive process. Drawing inspiration from supervised learning, researchers have explored offline RL as a means to circumvent the traditional paradigm of online interactions [11], [12]. Compared to online RL, offline RL more closely resembles a data-driven paradigm as it relies on the offline dataset. Various approaches of offline RL have been proposed, including methods based on value functions [12], [13], uncertainty quantification [14], [15], [16], dynamics estimation [17], [17], [18], [19], [20] and conditional behavior cloning that avoids value functions [21], [22], [23], [24], [25], [26], [27]. These investigations into offline RL have extensively explored the utilization of offline data, thereby stimulating further scholarly contemplation on leveraging such data for RL applications.

B. Sequence Modeling for Offline Reinforcement Learning

As supervised learning continues to evolve, sequence models have achieved significant success in many research areas. Given the structural similarities between RL’s Markov processes and sequence modeling, many researchers have begun to consider integrating sequence models with RL. The Decision Transformer (DT) [1] employs a Transformer to convert an RL problem into a sequence modeling task and treats a trajectory as a sequence of rewards, states, and actions. Max et al. [28] discuss the role of the attention mechanisms in DT, offering various opinions and motivating us to employ advanced sequence modeling techniques. Decision Convformer [29] incorporates discussions from the computer vision field about the MetaFormer [30] structure for transformers and proposes considerations for the use of local features. However, the structure in DC focuses too much on local information and structures, which can impact

the utilization of global information. Decision S4 [31] uses S4 layers for sequence modeling in offline RL. Decision Mamba [8] integrates the latest Mamba sequence model. However, both methods merely apply these new sequence models directly without further exploring and utilizing the potential of these sequence models. In this paper, we introduce MambaDM, an innovative sequence modeling framework designed for offline RL. MambaDM integrates the unique features of state space models to effectively combine local and global features, enhancing learning capabilities and efficiently handling larger-scale training.

III. PRELIMINARIES

A. RL Problem Setup

An RL problem can be modeled as a Markov decision process (MDP) $\mathcal{M} = \langle \rho_0, \mathcal{S}, \mathcal{A}, P, \mathcal{R}, \gamma \rangle$, where ρ_0 represents the initial state distribution, \mathcal{S} is the state space, and \mathcal{A} is the action space. At timestep t , a specific state and action are denoted by s_t and a_t , respectively. The transition probability $P(s_{t+1}|s_t, a_t)$ adheres to the Markov property. The reward function \mathcal{R} provides the reward $r_t = \mathcal{R}(s_t, a_t)$, and $\gamma \in (0, 1)$ is the discount factor. We utilize the return-to-go (RTG, i.e., $\hat{R}_t = \sum_{k=t}^{\infty} \gamma^k r_k$) as the reward input, following the approach of the Decision Transformer. Given an offline RL trajectory dataset, our objective is to determine an optimal policy π^* that predicts the best actions to maximize the expected return by interacting with the environment.

B. State Space Model and Mamba

The state space models (SSMs) are a recent class of sequence models inspired by a particular dynamic system. Concretely, we provide a detailed definition of structure state space models (S4) to illustrate the modeling process:

$$h'(t) = \mathbf{A}h(t) + \mathbf{B}x(t), \quad (1)$$

$$y(t) = \mathbf{C}h(t) + \mathbf{D}x(t), \quad (2)$$

where $(\mathbf{A}, \mathbf{B}, \mathbf{C}, \mathbf{D})$ controls the whole continuous system, and \mathbf{A} acts as an important state matrix which strongly decides the ability to capture long-range dependencies by different HIPPO initialization [32]. To operate discrete sequences, S4 needs to be transformed into a discretized form:

$$h'(t) = \bar{\mathbf{A}}h(t) + \bar{\mathbf{B}}x(t), \quad (3)$$

$$y(t) = \mathbf{C}h(t), \quad (4)$$

where S4 uses the zero-order hold (ZOH) discretization rule [33]. After transforming from $(\Delta, \mathbf{A}, \mathbf{B}, \mathbf{C}, \mathbf{D}) \mapsto (\bar{\mathbf{A}}, \bar{\mathbf{B}}, \mathbf{C})$, the model can be computed with linear recurrence view which only needs $O(1)$ complexity during inference, and can act as global convolution during training. This deformable nature gives SSM a remarkable lightweight advantage over classical sequence models [34], [35], [36], [37] in NLP tasks.

To further enhance selectivity and context-aware capabilities, Mamba [7] is proposed to handle complex sequence tasks by expanding the embedding space while maintaining efficient implementation. Building on the S4 structure,

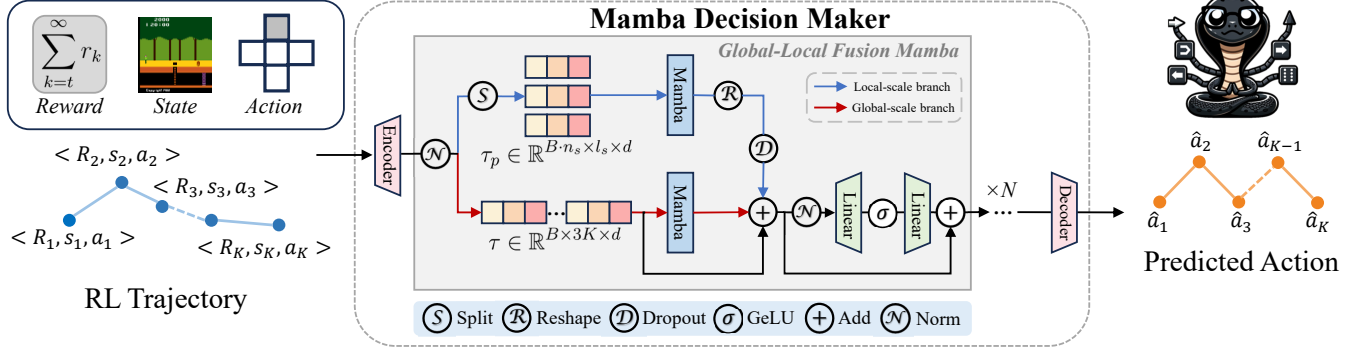


Fig. 1: **Overview of our proposed MambaDM.** The input RL trajectory is first processed by the embedding layers, and these embeddings are then passed through both local and global branches to extract multi-scale features. Subsequently, the combined information from these branches is fed into a feed-forward network (FFN). After passing through N layers, the final action sequence is obtained by the action predictor.

Mamba transitions the main parameters from time-invariant to time-varying. Additionally, the architecture of the Mamba block integrates elements from both H3 [38] and gated MLP [39], [40], making it versatile for incorporation into neural networks. Recent extensive research demonstrates that Mamba significantly contributes to various tasks, including but not limited to, vision [41], [42], [43], language [44], [45], and medical [46], [47] domains.

IV. METHODOLOGY

A. Overview

The overview of our method is presented in Fig. 1. We propose a global-local fusion mamba (GLOMa) framework where the input trajectory is processed jointly by multi-scale branches. This design ensures that both global and local features are effectively leveraged for optimal performance.

B. Motivation and Insights

As mentioned before, RL trajectories differ from conventional sequences with two unique properties: (1) local correlations and (2) global correlations. In this paper, we adopt the Mamba model [7], known for its efficient sequence modeling and strong ability to capture multi-scale dependencies [6], to explore its capability to model the inner relationship of RL trajectories. We develop the global-local fusion mamba (GLOMa) module to effectively integrate local features and global features. Inspired by transformer-in-transformer (TNT [48]), which aims to extract finer-grained features, GLOMa focuses on fusing global and local features within trajectories, differing from TNT's focus on combining with more granular image texture features.

C. Mamba Decision Maker

Global-local fusion Mamba (GLOMa). Given a sequence of trajectories τ_{raw} sampled from dataset D with raw RTG, state, and action, we first obtain the trajectory representation τ through the token embedding layer:

$$\tau = \text{Emb}(\tau_{\text{raw}}) = (\langle \hat{R}_1, s_1, a_1 \rangle, \dots, \langle \hat{R}_K, s_K, a_K \rangle), \quad (5)$$

where K is the context length, d is the embedding dimension. Then, the trajectory sequence τ is processed by both the global and local branches. For the local branch, the input sequence is evenly divided into sub-sequences, each of length l_s . Since the total sequence length is fixed with $3K$, it might lead to uneven sub-sequence lengths. To address this, we pad zeros at the end of the sequence to ensure uniform length and generate the sub-sequences through:

$$l_p = (l_s - (3K \bmod l_s)) \bmod l_s, \quad (6)$$

$$\tau_p = g_s(\text{Pad}(\tau, l_p), l_s) \in \mathbb{R}^{n_s \times l_s \times d}, \quad (7)$$

where l_p denotes the padding length, $n_s = \frac{3K+l_p}{l_s}$ denotes the number of sub-sequences. \bmod and Pad means the modulo and padding operator, respectively. $g_s(\cdot)$ denotes the split function, which splits the input into l_s -length sequences. The n_s dimension will be merged with the batch dimension during training. We can then obtain the local-scale feature of sub-sequences through the Mamba module by Eq. 8. For the global branch, we model the entire sequence directly using the Mamba block with Eq. 9. Overall, this multi-scale process can be formulated by:

$$f_{\text{local}} = \text{Mamba}(\text{LN}(\tau_p)), \quad (8)$$

$$f_{\text{global}} = \text{Mamba}(\text{LN}(\tau)), \quad (9)$$

where LN denotes the layer normalization. The multi-scale feature f_c is combined with a Dropout layer [49] and then fed into an FFN layer to obtain the output features:

$$f_c = f_{\text{global}} + \text{Dropout}(f_{\text{local}}), \quad (10)$$

$$f = \text{FFN}(\text{LN}(f_c)) + f_c. \quad (11)$$

After passing through L layers of the network, the final features f_L are input into the prediction head to predict the action sequence: $\hat{a}_t = \text{Head}(f_L)$ with $t = 1, 2, \dots, K$.

By implementing these techniques, our Global-local fusion mamba (GLOMa) framework aims to effectively capture and integrate both local and global features to better understand the inner correlations within RL trajectories, enhancing the model's ability to predict action sequences accurately.

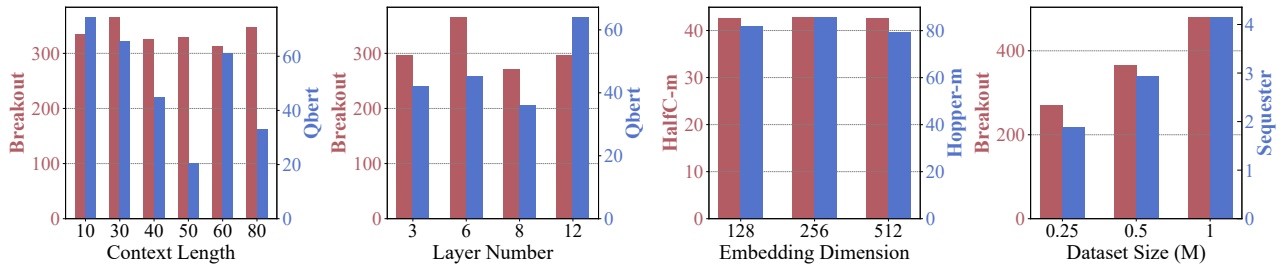


Fig. 2: **Visualization of the scaling factors impact on MambaDM’s performances in reinforcement learning tasks**, where color red and blue denote different RL domains. We find that MambaDM does not demonstrate a definitive scaling law when scaling the model size, but increasing the dataset size can significantly improve the model’s performance.

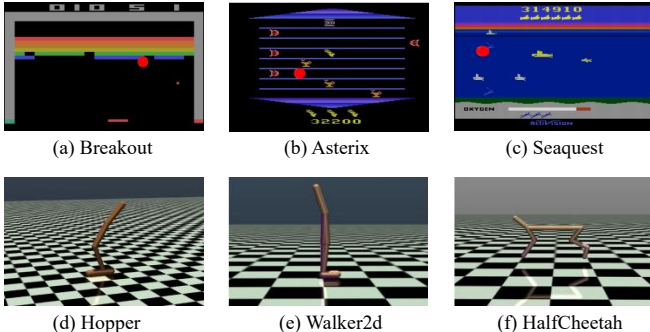


Fig. 3: **Visualization of RL benchmarks**, including Atari Games (a)-(c) and D4RL domains (d)-(f).

Training and Inference. In the training stage, considering the true-optimal action as a_t^* , the training object is to minimize the loss between the predicted action \hat{a}_t and true action a_t^* :

$$\mathcal{L} = \begin{cases} \mathbb{E}_{\tau_{\text{raw}} \sim D} [\|a_t^* - \hat{a}_t\|^2], & \text{if action is continuous;} \\ \mathbb{E}_{\tau_{\text{raw}} \sim D} [-a_t^* \log(\hat{a}_t)], & \text{if action is discrete.} \end{cases} \quad (12)$$

In this paper, the actions in the Atari benchmark [50] are discrete, whereas those in D4RL [51] are continuous. During inference, the final action a_K is unknown. To handle the variable length of the input sequence, we set l_s to match its length. Additionally, the true RTG is unavailable. Therefore, following [1], we set the target RTG to be the initial RTG. We find that the initial RTG significantly affects the final results, and we discuss this phenomenon in Sec. V-F.

V. EXPERIMENTS

A. Exploring the Scaling Laws of MambaDM

In this section, we investigate the scaling laws of MambaDM within the context of reinforcement learning (RL) tasks. Scaling laws [52], as observed in the natural language processing (NLP) domain, suggest that increasing computational resources generally leads to improved performance. Our objective is to explore if similar scaling laws apply to MambaDM when used for RL tasks.

Experiment Setting. To systematically study this, we conduct a series of experiments varying key parameters of MambaDM. Specifically, we manipulate the context length, layer number, embedding dimension, and dataset size. The settings

Scaling Factor	Context Length	Layer Number	Embedding Dimension	Dataset Size
Range	(10, 30, 50, 80, 100)	(3, 6, 8, 12)	(128, 256, 512)	(0.25M, 0.5M, 1M)

TABLE I: **Experimental settings for scaling factors.**

for these parameters are chosen to cover a broad range of values and to provide a comprehensive understanding of their impact on performance. The details of these settings are illustrated in Tab. I.

Discussion. In our investigation of the scaling law in MambaDM for RL tasks, we explore how variations in scaling factors affect performance, as depicted in Fig. 2. Our findings indicate that MambaDM does not exhibit NLP-like scaling behaviors in Atari and OpenAI Gym. As we increase the model size, performance fluctuations are observed instead of a clear upward trend. Consequently, **MambaDM does not demonstrate a definitive scaling law when scaling the model size.** However, our experiments show that **increasing the dataset size can significantly improve the model’s performance.** This suggests that focusing on gathering larger and more diverse RL datasets could be a more effective strategy for enhancing performance compared to merely increasing the model size in Atari and OpenAI Gym.

We delve into the reasons why MambaDM does not exhibit an NLP-like scaling law with several points: (1) The model size is strongly correlated with its capability, but the optimal model size varies across different RL tasks. Our experiments are limited to two standard RL datasets, which may not provide a comprehensive understanding of scaling behavior across diverse RL tasks. (2) RL trajectories possess different attributes compared to text data, despite Mamba showing scaling law behaviors in NLP tasks [7]. (3) Increasing the dataset size enhances model performance. This empirical conclusion aligns with findings from existing studies [53], [54]. Overall, exploring scaling law in RL remains a worthwhile direction.

B. Evaluations on Atari Games

Baselines. We choose six models as our baselines, including temporal difference learning methods: Conservative Q-Learning (CQL [13]), imitation learning methods: Behavior Cloning (BC [56]), Decision Transformer (DT [1]) and its variants: Decision ConvFormer (DC [29]) and Decision Mamba (DMamba [8]).

Experiment Setting. To ensure a fair comparison, we adopt the same model hyperparameter settings as those used in DT

Game	CQL	BC	DT	DC	DC ^{hybrid}	DMamba [†]	MambaDM
Breakout	211.1	142.7	242.4 ± 31.8	352.7 ± 44.7	416.0 ± 105.4	239.2 ± 26.4	365.4 ± 20.0
Qbert	104.2	20.3	28.8 ± 10.3	67.0 ± 14.7	62.6 ± 9.4	42.3 ± 8.5	74.4 ± 8.4
Pong	111.9	76.9	105.6 ± 2.9	106.5 ± 2.0	111.1 ± 1.7	63.2 ± 102.1	110.8 ± 2.3
Seaquest	1.7	2.2	2.7 ± 0.7	2.6 ± 0.3	2.7 ± 0.04	2.2 ± 0.03	2.9 ± 0.1
Asterix	4.6	4.7	5.2 ± 1.2	6.5 ± 1.0	6.3 ± 1.8	5.5 ± 0.3	7.5 ± 1.4
Frostbite	9.4	16.1	25.6 ± 2.1	27.8 ± 3.7	28.0 ± 1.8	25.3 ± 1.5	33.7 ± 4.4
Assault	73.2	62.1	52.1 ± 36.2	73.8 ± 20.3	79.0 ± 13.1	67.2 ± 6.9	81.4 ± 3.1
Gopher	2.8	33.8	34.8 ± 10.0	52.5 ± 9.3	51.6 ± 10.7	27.0 ± 3.9	54.4 ± 11.1

TABLE II: **Comparisons results of MambaDM and baselines in Atari.** The gamer-normalized returns are reported, following [55], and averaged across three random seeds. The top-1 and top-2 results among the DT variants are highlighted in **deep pink** and **light pink**, respectively. [†] denotes that we reproduce the DMamba’s results of the last four games (in gray) which are not provided in the origin paper.

Dataset	Env.	TD3+BC	IQL	CQL	RvS	DT	DS4	DMamba	MambaDM
<i>M</i>	halfcheetah	48.3	47.4	44.0	41.6	42.6	42.5	42.8	42.8 ± 0.1
	hopper	59.3	63.8	58.5	60.2	68.4	54.2	83.5	85.7 ± 7.8
	walker2d	83.7	79.9	72.5	71.7	75.5	78.0	78.2	78.2 ± 0.6
<i>M-R</i>	halfcheetah	44.6	44.1	45.5	38.0	37.0	15.2	39.6	39.1 ± 0.1
	hopper	60.9	92.1	95.0	73.5	85.6	49.6	82.6	86.1 ± 2.5
	walker2d	81.8	73.7	77.2	60.6	71.2	69.0	70.9	73.4 ± 2.6
<i>M-E</i>	halfcheetah	90.7	86.7	91.6	92.2	88.8	92.7	91.9	86.5 ± 1.2
	hopper	98.0	91.5	105.4	101.7	109.6	110.8	111.1	110.5 ± 0.3
	walker2d	110.1	109.6	108.8	106.0	109.3	105.7	108.3	108.8 ± 0.1

TABLE III: **Comparisons results of MambaDM and baselines in D4RL benchmark.** We report the expert-normalized returns, following [51], averaged across three random seeds. The top-1 and top-2 results among the DT variants are colored in **deep pink** and **light pink**, respectively.

and DC. The experimental results for the baselines are from DC and DMamba. Each experimental result is the average of three runs with different random seeds. We conduct eight discrete control tasks from the Atari domain, where some domains are illustrated in Fig. 3. Each experiment is conducted on a single NVIDIA 4090 GPU.

Comparisons with the State-of-the-art. As illustrated in Tab. II, our proposed MambaDM has a significant improvement across different Atari games. For instance, MambaDM’s performance on Qbert significantly improved by 45.6% and 32.1% compared with DT and DMamba. When compared with the latest state-of-the-art method DC, MambaDM achieves favorable gains across all games. These results demonstrate the effectiveness of our method in the discrete Atari domain.

C. Evaluations on OpenAI Gym

Baselines. Seven models are chosen as our baselines, including TD3+BC [57], IQL [58], RvS [27], DT [1] and two state space model-based [6] approaches: DS4 [31] and DMamba [8].

Experiment Setting. We adopt the same hyperparameter settings as those used in DT and DC for fair comparisons. We conduct experiments in three MuJoCo domains [51]: halfcheetah, hopper, and walker (Fig. 3), where each domain has three quality levels, including medium (M), medium-replay (M-R) and medium-expert (M-E).

Comparisons with the State-of-the-art. Tab. III presents a performance comparison of MambaDM against several baselines in the D4RL benchmark. MambaDM consistently

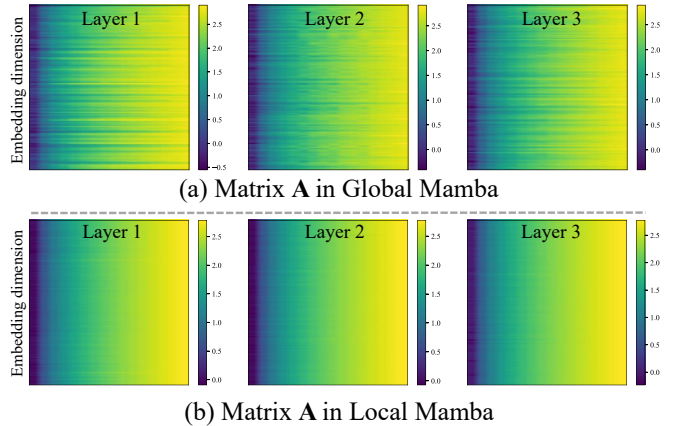


Fig. 4: **Visualization of the eigenvalues in the core matrices A of our proposed GLoMA,** including eigenvalues in (a) global mamba and (b) local mamba matrices.

demonstrates superior performance, often securing top-1 and top-2 rankings in various environments. For instance, in the hopper (M) dataset, MambaDM achieves an average return of 85.7, significantly outperforming DT (68.4) and DS4 (54.2). These results underscore MambaDM’s ability to consistently outperform or closely match the top-performing baselines across diverse datasets and tasks, demonstrating its reliability and robustness in continuous RL environments.

D. Analysis of the Learned Dependencies in MambaDM

It is important to note that in state-space models, \bar{A} is defined as a transition matrix parameterized by A and Δ , with A playing a critical role in influencing the stability of the dynamic system [6], [32]. The magnitude of the eigenvalues in A , $|\lambda_j|$, is pivotal in determining the range of dependencies captured by the model. If $|\lambda_j| \geq 1$, the model can retain historical information across numerous time steps, effectively capturing long-range dependencies. Conversely, when $|\lambda_j|$ is significantly less than 1, the historical information decays rapidly, leading to a focus on short-term dependencies.

We visualize the key transition matrix A in the Mamba block under the Atari domain. For simplified visualization, the eigenvalues of A are presented in log-scale. Our analysis reveals two key findings: (1) The distribution of eigenvalues in the Global Mamba varies significantly across different embedding dimensions. As the layers deepen, there is a noticeable trend of increasing eigenvalues, indicating enhanced preservation of long-range information, indicating that long-range information is progressively preserved and accentuated as the network depth increases. (2) The eigenvalues in the Local Mamba exhibit a stable distribution across different embedding dimensions and layers, suggesting that the Local Mamba effectively captures both short-range and long-range dependencies, maintaining a balanced weight distribution between them. In summary, Fig. 4 illustrates how different scale (*i.e.*, global or local) blocks handle varying ranges of dependencies. This highlights the complementary roles of

Method	Type	Module	Breakout	Qbert	Sequest	Pong
CMC	Cascaded	Mamba & Conv	330.3 ±78.8	21.5 ±5.5	63.4 ±13.7	1.4 ±0.1
PMC	Parallel	Mamba & Conv	298.6 ±81.7	21.6 ±7.6	13.0 ±3.8	2.7 ±0.1
GLoMa (ours)	Parallel	Mamba only	365.4 ±20.0	74.4 ±8.4	110.8 ±2.3	2.9 ±0.1

TABLE IV: **Ablation results of Mamba module combinations.** We set up three kinds of mamba methods including Cascaded Mamba-Conv (CMC), Parallel Mamba-Conv (PMC), and our proposed GLoMa.

A_n Initialization	Breakout	Sequest
$A_n = -1/2$	329.8	3.1
$A_n = -(n+1)$	365.4	2.9

TABLE V: **Ablation results of different initialization of Mamba matrix A_n .**

Context length	10	30	40	60	Mean
DMamba	231.6	239.2	295.9	271.1	259.5
MambaDM	334.4	365.4	325.7	313.2	334.7 (+75.2)

TABLE VI: **Ablation results of different context length K in Atari Breakout.**

global and local Mamba blocks in processing and preserving multi-scale information within the model.

E. Exploration on Mamba Module Combinations.

To design a robust and effective module, we implemented two methods with different embedding configurations (cascaded/parallel) and sub-module choices (mamba/convolution). Results in Tab. IV show that GLoMa significantly outperforms both CMC and PMC on the Atari datasets, confirming the robustness of our GLoMa design. The analysis of module design is discussed as follows.

Our model is designed with a parallel architecture that includes a global branch and a local branch. The global branch extracts global information within the RL trajectory, while the local branch focuses on local information based on MDP. To better validate the effectiveness of our design, we tried some other reasonable modules. As claimed in the DC [29], due to the MDP, the current and previous features are critical and convolutional operations can effectively extract such local information. Therefore, we replaced our local branch with the convolutional module from DC to create the Parallel Mamba-Conv (PMC). However, as shown in Tab. IV, PMC did not yield satisfactory results, demonstrating that the convolutional operation is not suited to extract local features when cooperating with Mamba. Additionally, considering that the processing order may affect performance, we designed a coarse-to-fine cascaded Mamba-Conv (CMC) structure. This approach aimed to first extract global features and then refine local features, but the results for CMC were also suboptimal. Our proposed GLoMa module is specifically tailored for capturing the global and local correlations to better understand the inner relationships in RL trajectories. Therefore, our module design is well-justified, and the results in the main text indicate that our model achieved the best performance, thereby demonstrating its effectiveness.

Atari	Init RTG	Breakout				Qbert				Pong			
		45	90	900	1800	1000	2500	10000	14000	10	20	100	1000
	Score	194.5	300.3	365.3	337.0	24.4	25.4	45.4	38.6	87.2	106.2	110.8	107.6
OpenAI Gym	Init RTG	Halfcheetah-M				Hopper-M				Walker2d-M			
		2500	5000	10000	50000	1800	3600	7200	36000	6000	12000	24000	240000
	Score	75.3	77.3	78.2	76.9	58.0	81.2	84.9	85.7	42.6	42.8	42.7	42.8

TABLE VII: **Ablation results of MambaDM with different initialized RTG.**

F. Ablation Studies

Ablations on Mamba initialization. As demonstrated by [32], [6], the initialization of the state matrix A_n significantly influences the stability of overall performance, as the eigenvalues of A_n are closely related to the information transformation process. Consequently, we conduct experiments by varying the initial values of A_n . The results presented in Tab. V indicate that our MambaDM exhibits stable performance across different initializations.

Evaluating with different context length. Mamba has demonstrated strong stability in handling long sequences within NLP tasks [7]. To verify the stability of our proposed method, we evaluate the effect of context length K compared to DMamba. The results in Tab. VI reveal that MambaDM not only maintains stable performance across various context lengths K , but also achieves significantly improved results, with an average increase of 75.2 points compared to DMamba.

Ablations on different initialized RTG. Tab. VII explores the impact of different initial return-to-go (RTG) settings on the final performance across various datasets. The results indicate that, generally, as the initial RTG increases, the overall performance of the model improves. However, an excessively high initial RTG can negatively affect results (e.g., in Breakout). Overall, the performance of the model is highly correlated with the initial RTG, showing a positive relationship within a certain range. This suggests that while increasing RTG can enhance performance, there is a threshold beyond which the benefits diminish or even reverse. Efficiently determining the optimal RTG setting to avoid extensive experimentation and to enable the model to achieve the best performance is a pertinent area for future research.

VI. CONCLUSION

In this study, we proposed the Mamba Decision Maker (MambaDM), a novel action predictor designed to capture multi-scale features and better understand the correlations within RL trajectories. MambaDM leverages a unique global-local fusion mamba (GLoMa) mixer module that adeptly integrates global and local features of input sequences. Extensive experiments have demonstrated that MambaDM achieves state-of-the-art performance on Atari and OpenAI Gym benchmarks. Moreover, our investigation into the scaling laws of MambaDM reveals that increasing the dataset size results in significant performance improvements, underscoring the importance of dataset size over model size in enhancing performance. In summary, MambaDM presents a promising alternative for sequence modeling in RL, offering efficient multi-scale dependency modeling and paving the way for future advancements in the field.

REFERENCES

- [1] L. Chen, K. Lu, A. Rajeswaran, K. Lee, A. Grover, M. Laskin, P. Abbeel, A. Srinivas, and I. Mordatch, "Decision transformer: Reinforcement learning via sequence modeling," *NeurIPS*, vol. 34, pp. 15 084–15 097, 2021.
- [2] P.-L. Guhur, S. Chen, R. G. Pinel, M. Tapaswi, I. Laptev, and C. Schmid, "Instruction-driven history-aware policies for robotic manipulations," in *CoRL*. PMLR, 2023, pp. 175–187.
- [3] M. Shridhar, L. Manuelli, and D. Fox, "Perceiver-actor: A multi-task transformer for robotic manipulation," in *CoRL*. PMLR, 2023, pp. 785–799.
- [4] D. Shah, A. Bhorkar, H. Leen, I. Kostrikov, N. Rhinehart, and S. Levine, "Offline reinforcement learning for customizable visual navigation," in *NeurIPS Workshops*, 2022.
- [5] S. Lifshitz, K. Paster, H. Chan, J. Ba, and S. McIlraith, "Steve-1: A generative model for text-to-behavior in minecraft," *NeurIPS*, vol. 36, 2024.
- [6] A. Gu, K. Goel, and C. Re, "Efficiently modeling long sequences with structured state spaces," in *ICLR*, 2021.
- [7] A. Gu and T. Dao, "Mamba: Linear-time sequence modeling with selective state spaces," *arXiv preprint arXiv:2312.00752*, 2023.
- [8] T. Ota, "Decision mamba: Reinforcement learning via sequence modeling with selective state spaces," *arXiv preprint arXiv:2403.19925*, 2024.
- [9] R. S. Sutton and A. G. Barto, "Reinforcement learning: An introduction," *Robotica*, vol. 17, no. 2, pp. 229–235, 1999.
- [10] —, "The reinforcement learning problem," *Reinforcement learning: An introduction*, pp. 51–85, 1998.
- [11] S. Levine, A. Kumar, G. Tucker, and J. Fu, "Offline reinforcement learning: Tutorial, review," and *Perspectives on Open Problems*, vol. 5, 2020.
- [12] S. Fujimoto, D. Meger, and D. Precup, "Off-policy deep reinforcement learning without exploration," in *ICML*. PMLR, 2019, pp. 2052–2062.
- [13] A. Kumar, A. Zhou, G. Tucker, and S. Levine, "Conservative q-learning for offline reinforcement learning," *NeurIPS*, vol. 33, pp. 1179–1191, 2020.
- [14] R. Agarwal, D. Schuurmans, and M. Norouzi, "An optimistic perspective on offline reinforcement learning," in *ICML*. PMLR, 2020, pp. 104–114.
- [15] Y. Wu, S. Zhai, N. Srivastava, J. Susskind, J. Zhang, R. Salakhutdinov, and H. Goh, "Uncertainty weighted actor-critic for offline reinforcement learning," *arXiv preprint arXiv:2105.08140*, 2021.
- [16] T. Yu, G. Thomas, L. Yu, S. Ermon, J. Y. Zou, S. Levine, C. Finn, and T. Ma, "Mopo: Model-based offline policy optimization," *NeurIPS*, vol. 33, pp. 14 129–14 142, 2020.
- [17] R. Kidambi, A. Rajeswaran, P. Netrapalli, and T. Joachims, "Morel: Model-based offline reinforcement learning," *NeurIPS*, vol. 33, pp. 21 810–21 823, 2020.
- [18] A. Argenson and G. Dulac-Arnold, "Model-based offline planning," *arXiv preprint arXiv:2008.05556*, 2020.
- [19] S. Depeweg, J. M. Hernández-Lobato, F. Doshi-Velez, and S. Udluft, "Learning and policy search in stochastic dynamical systems with bayesian neural networks," *arXiv preprint arXiv:1605.07127*, 2016.
- [20] P. Swainna, S. Udluft, and T. Runkler, "Overcoming model bias for robust offline deep reinforcement learning," *Engineering Applications of Artificial Intelligence*, vol. 104, p. 104366, 2021.
- [21] Y. Ding, C. Florensa, P. Abbeel, and M. Phielipp, "Goal-conditioned imitation learning," *NeurIPS*, vol. 32, 2019.
- [22] D. Ghosh, A. Gupta, A. Reddy, J. Fu, C. Devin, B. Eysenbach, and S. Levine, "Learning to reach goals via iterated supervised learning," *arXiv preprint arXiv:1912.06088*, 2019.
- [23] C. Lynch, M. Khansari, T. Xiao, V. Kumar, J. Tompson, S. Levine, and P. Sermanet, "Learning latent plans from play," in *CoRL*. PMLR, 2020, pp. 1113–1132.
- [24] A. Kumar, X. B. Peng, and S. Levine, "Reward-conditioned policies," *arXiv preprint arXiv:1912.13465*, 2019.
- [25] J. Schmidhuber, "Reinforcement learning upside down: Don't predict rewards—just map them to actions," *arXiv preprint arXiv:1912.02875*, 2019.
- [26] R. K. Srivastava, P. Shyam, F. Mutz, W. Jaśkowski, and J. Schmidhuber, "Training agents using upside-down reinforcement learning," *arXiv preprint arXiv:1912.02877*, 2019.
- [27] S. Emmons, B. Eysenbach, I. Kostrikov, and S. Levine, "Rvs: What is essential for offline rl via supervised learning?" *ICLR*, 2021.
- [28] M. Siebenborn, B. Belousov, J. Huang, and J. Peters, "How crucial is transformer in decision transformer?" *arXiv preprint arXiv:2211.14655*, 2022.
- [29] J. Kim, S. Lee, W. Kim, and Y. Sung, "Decision convformer: Local filtering in metaformer is sufficient for decision making," in *ICLR*, 2023.
- [30] W. Yu, M. Luo, P. Zhou, C. Si, Y. Zhou, X. Wang, J. Feng, and S. Yan, "Metaformer is actually what you need for vision," in *CVPR*, 2022, pp. 10 819–10 829.
- [31] S. B. David, I. Zimerman, E. Nachmani, and L. Wolf, "Decision s4: Efficient sequence-based rl via state spaces layers," in *ICLR*, 2022.
- [32] A. Gu, T. Dao, S. Ermon, A. Rudra, and C. Ré, "Hippo: Recurrent memory with optimal polynomial projections," *NeurIPS*, vol. 33, pp. 1474–1487, 2020.
- [33] A. Gu, K. Goel, and C. Re, "Efficiently modeling long sequences with structured state spaces," in *(ICLR)*, 2021.
- [34] A. Vaswani, N. Shazeer, N. Parmar, J. Uszkoreit, L. Jones, A. N. Gomez, Ł. Kaiser, and I. Polosukhin, "Attention is all you need," *NeurIPS*, vol. 30, 2017.
- [35] T. Dao, D. Fu, S. Ermon, A. Rudra, and C. Ré, "Flashattention: Fast and memory-efficient exact attention with io-awareness," *NeurIPS*, vol. 35, pp. 16 344–16 359, 2022.
- [36] T. Dao, "Flashattention-2: Faster attention with better parallelism and work partitioning," *ICLR*, 2023.
- [37] B. Peng, E. Alcaide, Q. Anthony, A. Albalak, S. Arcadinho, S. Biderman, H. Cao, X. Cheng, M. Chung, L. Derczynski *et al.*, "Rwkv: Reinventing rns for the transformer era," in *EMNLP Findings*, 2023, pp. 14 048–14 077.
- [38] D. Y. Fu, T. Dao, K. K. Saab, A. W. Thomas, A. Rudra, and C. Re, "Hungry hungry hippos: Towards language modeling with state space models," in *ICLR*, 2022.
- [39] H. Touvron, T. Lavril, G. Izacard, X. Martinet, M.-A. Lachaux, T. Lacroix, B. Rozière, N. Goyal, E. Hambro, F. Azhar *et al.*, "Llama: Open and efficient foundation language models," *arXiv preprint arXiv:2302.13971*, 2023.
- [40] A. Chowdhery, S. Narang, J. Devlin, M. Bosma, G. Mishra, A. Roberts, P. Barham, H. W. Chung, C. Sutton, S. Gehrmann *et al.*, "Palm: Scaling language modeling with pathways," *JMLR*, vol. 24, no. 240, pp. 1–113, 2023.
- [41] L. Zhu, B. Liao, Q. Zhang, X. Wang, W. Liu, and X. Wang, "Vision mamba: Efficient visual representation learning with bidirectional state space model," *arXiv preprint arXiv:2401.09417*, 2024.
- [42] Y. Liu, Y. Tian, Y. Zhao, H. Yu, L. Xie, Y. Wang, Q. Ye, and Y. Liu, "Vmamba: Visual state space model," *arXiv preprint arXiv:2401.10166*, 2024.
- [43] Y. Teng, Y. Wu, H. Shi, X. Ning, G. Dai, Y. Wang, Z. Li, and X. Liu, "Dim: Diffusion mamba for efficient high-resolution image synthesis," *arXiv preprint arXiv:2405.14224*, 2024.
- [44] M. Pióro, K. Ciebiera, K. Król, J. Ludziejewski, and S. Jaszczur, "Moe-mamba: Efficient selective state space models with mixture of experts," *ICLR Workshops*, 2024.
- [45] Q. Anthony, Y. Tokpanov, P. Glorioso, and B. Millidge, "Black-mamba: Mixture of experts for state-space models," *arXiv preprint arXiv:2402.01771*, 2024.
- [46] J. Liu, H. Yang, H.-Y. Zhou, Y. Xi, L. Yu, Y. Yu, Y. Liang, G. Shi, S. Zhang, H. Zheng *et al.*, "Swin-umamba: Mamba-based unet with imagenet-based pretraining," *arXiv preprint arXiv:2402.03302*, 2024.
- [47] Z. Xing, T. Ye, Y. Yang, G. Liu, and L. Zhu, "Segmamba: Long-range sequential modeling mamba for 3d medical image segmentation," *arXiv preprint arXiv:2401.13560*, 2024.
- [48] K. Han, A. Xiao, E. Wu, J. Guo, C. Xu, and Y. Wang, "Transformer in transformer," *NeurIPS*, vol. 34, pp. 15 908–15 919, 2021.
- [49] N. Srivastava, G. Hinton, A. Krizhevsky, I. Sutskever, and R. Salakhutdinov, "Dropout: a simple way to prevent neural networks from overfitting," *JMLR*, vol. 15, no. 1, pp. 1929–1958, 2014.
- [50] V. Mnih, K. Kavukcuoglu, D. Silver, A. Graves, I. Antonoglou, D. Wierstra, and M. Riedmiller, "Playing atari with deep reinforcement learning," *arXiv preprint arXiv:1312.5602*, 2013.
- [51] J. Fu, A. Kumar, O. Nachum, G. Tucker, and S. Levine, "D4rl: Datasets for deep data-driven reinforcement learning," *arXiv preprint arXiv:2004.07219*, 2020.
- [52] J. Kaplan, S. McCandlish, T. Henighan, T. B. Brown, B. Chess, R. Child, S. Gray, A. Radford, J. Wu, and D. Amodei, "Scaling laws for neural language models," *arXiv preprint arXiv:2001.08361*, 2020.

- [53] L. Gao, J. Schulman, and J. Hilton, "Scaling laws for reward model overoptimization," in *International Conference on Machine Learning*. PMLR, 2023, pp. 10 835–10 866.
- [54] P. Bhargava, R. Chitnis, A. Geramifard, S. Sodhani, and A. Zhang, "When should we prefer decision transformers for offline reinforcement learning?" in *ICLR*, 2024. [Online]. Available: <https://openreview.net/forum?id=vpV7fOFQy4>
- [55] W. Ye, S. Liu, T. Kurutach, P. Abbeel, and Y. Gao, "Mastering atari games with limited data," *NeurIPS*, vol. 34, pp. 25 476–25 488, 2021.
- [56] M. Bain and C. Sammut, "A framework for behavioural cloning." in *Machine Intelligence*, 1995, pp. 103–129.
- [57] S. Fujimoto and S. S. Gu, "A minimalist approach to offline reinforcement learning," *NeurIPS*, vol. 34, pp. 20 132–20 145, 2021.
- [58] I. Kostrikov, A. Nair, and S. Levine, "Offline reinforcement learning with implicit q-learning," in *ICLR*, 2021.